CRITERIA FOR MINIMISING TRANSIENT STRESS IN CONVEYOR BELTS

A. Harrison
CSIRO Division of Applied Physics
Sydney, Australia 2070.

1. SUMMARY

Several mechanisms lead to the generation of elastic or stress waves in conveyor belts during starting and stopping. A model is described to explain the evolution of stresses in belts using solutions to the one-dimensional elastic wave equation. Techniques have been developed to measure and analyse these transient stresses in the belt using belt velocity characteristics. A close look at the methods presently employed to start and stop belts leads to new design criteria, which if implemented, will result in significant reduction in transient stress levels and so will allow a reduction in belt safety factors to near 3:1. This results in a lower installed belt cost.

2. Introduction

At present the required breaking strength of a steel-cord belt is determined by applying the desired operating factor of safety (f.o.s.), which typically has a value of ten, to the peak steady-state tension in the running loaded belt. Such a high f.o.s. value is considered to be necessary to overcome transient stresses in the belt during starting and stopping. The high cost of the belt in most conveyor installations reflects these high f.o.s. values.

A reduction in the f.o.s. can be achieved by reducing the transient stress in the belt caused by jerk or shock. One way of reducing the jerk in the belt is to reduce the rate of change of belt acceleration and deceleration (jerk) by controlled starting and braking of the drive to the belt. This paper describes some of the drive methods in use and for each drive system gives typical belt speed characteristics. An improved method for starting and stopping which will minimise belt acceleration and jerk is described.

3. Belt Stresses

A conveyor belt is always pretensioned. During the start or brake period, a dynamic loading is induced in the belt from shock generated by the drive-drum motion. Tension perturbations of this type are in fact travelling compressions and rare-factions in the belt, and lead to high belt stresses. The elastic wave of tension or compression travelling at the speed of sound in the belt exerts a stress on each belt element. These waves can snap the belt, cause splices to pull apart and destroy terminal pulley bearings.

These problems are overcome by using very high f.o.s. values on all components - at a great cost. Tension perturbations also excite the belt to flap transversely by the mechanism of parametric excitation. The natural frequency of the belt will be excited when the tension perturbation is at twice the belt frequency. These vibrations lead to idler bearing failure and high-frequency alternation in splice shear stresses which can lead to failure.

Figure 1 illustrates the various excitation paths that can lead to high belt stresses.

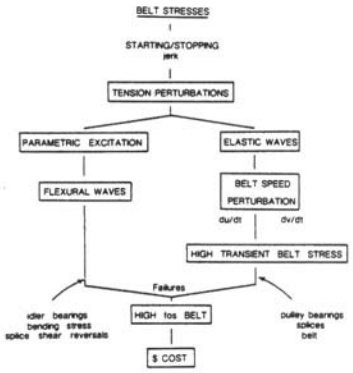

Fig. 1. Mechanisms leading to high transient stresses in conveyor belts.

4. Belt Oscillations

During the starting and stopping operation there are two distinctly different mechanisms that cause perturbations to the belt speed and belt tension in the longitudinal direction, namely circulating elastic waves and long period mass-spring oscillations of the whole system.

4.1 Elastic waves

Firstly, there are periodic variations in the belt speed at a location x along the belt due to travelling longitudinal or elastic waves. These waves are generated in both sides of the belt due to its interaction with the drive drum.

In the tight-side of the belt a tension wavefront is propagated following a belt jerk, and in the return side a compression wave is generated. Both travelling waves circulate, cross through one another, and eventually decay in amplitude. The variation in belt speed at the drum is due to the periodic arrival of compressed and elongated belt. Fig. 2 illustrates a belt model using a mass-spring system to include the initiation of elastic (stress) waves during transient operation. In the belt equivalent model, the take-up mass is permanently displaced at t = ∞ resulting in the well known tensions in the carrying and return span.

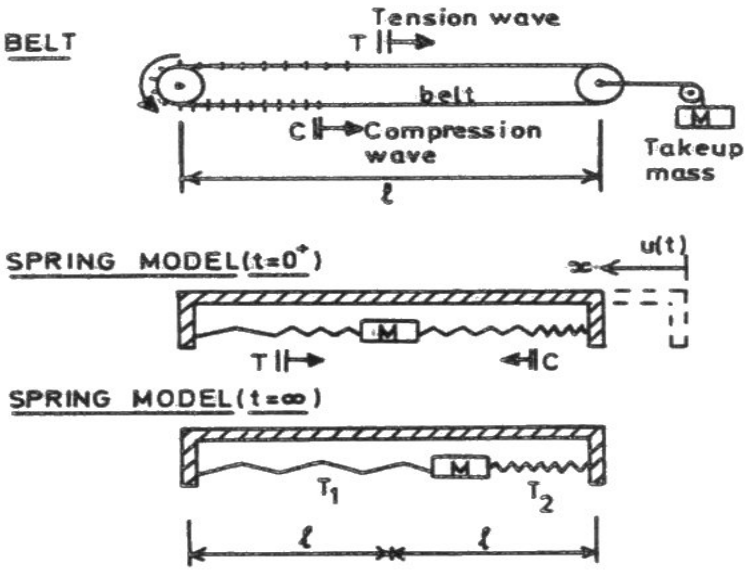

Fig. 2. Conveyor belt mass-spring model
showing transient and steady-state behaviour

The elastic waves cause a sinusoidally varying perturbation of the belt velocity, and satisfy the elastic wave equation for the belt

$$\frac{\partial^2 u}{\partial x^2} = \frac{1}{V_o^2} \cdot \frac{\partial^2 u}{\partial t^2} \qquad (1)$$

where u = U(x,t) is the longitudinal displacement of a small element of the belt at position x with time (1). The elastic wave velocity Vo may be calculated from the expression

$V_o = V_s$. Sq route $\rho_s/(\rho_b + \rho_i + \rho_m)$ (2)

where V_s is the speed of sound in a steel cord ~4.34 km/s, ρ is the mass/unit length and subscripts s, b, i and m refer to steel cord, belt, equivalent rotating parts and materials being conveyed respectively. Elastic waves with a wave velocity V_o of typically ~2 km/s lead to very high transient stresses in the plane of the belt. The stress in the belt at any location x varies sinusoidally with a period of $t_1 = 2\ell/V_o$ where ℓ is the conveyor belt length between terminal pulleys.

It is necessary to solve the wave equation for a conveyor belt so that a solution is available for a later calculation. A general solution for equation (1) is the sum of all harmonically related functions

$$u(x,t) = \sum_m u_o \cos\frac{m\pi x}{2\ell} \cdot \sin \omega t \qquad (3)$$

where u_o is an initial displacement, 'm' is a mode number, ℓ the belt length and ω the wave frequency in the belt. Differentiating equation (3) with respect to time yields the velocity mode for the belt, and for a fundamental mode (m=l), and $\omega = \pi V_o/\ell$,

$$\frac{\partial u}{\partial t}(x,t) = v(x,t) = V_o \cos\frac{\pi x}{2\ell} \cdot \cos \omega t \qquad (4)$$

where equation (4) satisfies the boundary conditions for the model in fig. 1, namely

$$V(o,o) = -V(2\ell,o) = V_o$$
$$V(2\ell,o) = V(\ell, {}^{\ell}/V_o) = o \qquad (5)$$

Using equation (4), it is possible to determine the effective belt mass m* that actually impedes the wave. The kinetic energy averaged over 1 cycle of the wave (3), with m=1 and the wave period $T = 4l/V_o$, is

$$K.E. = 1/\pi \int_o^{\pi} \int_{-\ell}^{\ell} \tfrac{1}{2} \mu . v(x,t)^2 . dx . d(\omega t)$$
$$= \tfrac{1}{2} . (\mu . 2\ell/4) . v_o^2 = \tfrac{1}{2}(m/4) . v_o^2 = \tfrac{1}{2} m^* . v_o^2 \qquad (6)$$

where μ is the belt mass/unit length, and M is the total belt mass impeding the wavefront. It is obvious that the effective mass M* = M/4 for the fundamental mode of longitudinal vibration.

4.2 Mass spring effect

A second source of perturbation to the belt velocity at a location x along the belt is a long period (> 10 s) damped oscillation attributed to the "mass-spring" effect (2). This effect is a mechanical vibration due to the interaction between the belt with stiffness k and the inertia of the take-up mass M¹. The natural mass-spring period of the damped belt spring system is

$$t_2 = 2\pi Sq\ route(M^1 + 1/3m)/k \qquad (7)$$

where m is the total belt mass including the mass equivalent of the rotating parts (idlers and pulleys) and the material load. Generally, t_2 is up to 10 times that of the decaying periodic stress wave period t_1 and contributes little to the belt stress.

Figure 3 summarises both types of longitudinal belt oscillations that result from a drive displacement. The long-term nature of the mass-spring effect is neglected in the calculation of transient stress since in practice the effect is very small compared to that from the elastic wave.

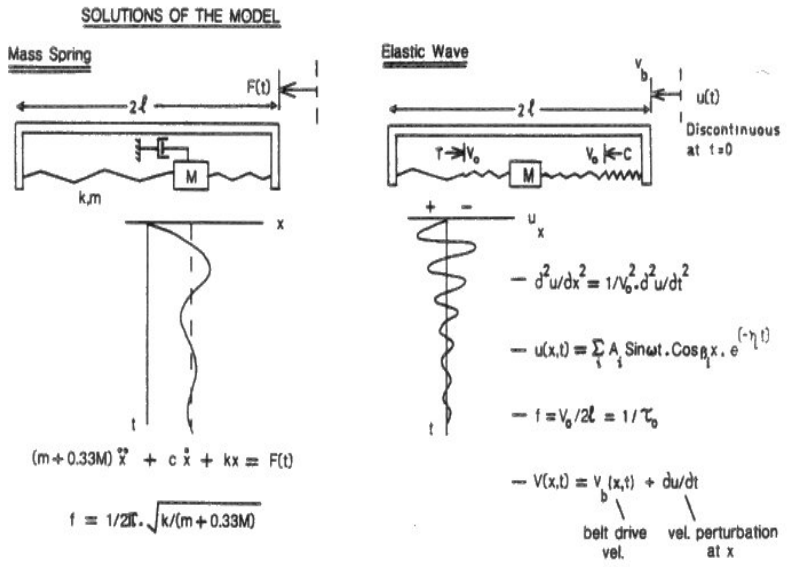

Fig. 3. Mass-spring and elastic wave oscillations for the belt

model in fig.1.

4.3 Belt velocity-time characteristics

The instantaneous belt velocity V_b (x,t) is given by

$$V_b(x,t) = V_d(x,t) + \frac{2u}{2t}\ (x,t) \qquad (8)$$

where $V_d(x,t)$ is the drive input velocity. Since the dynamic velocity component 2u/2t is non-zero in the starting and stopping period, the instantaneous belt acceleration is dependent upon the value of 2u/2t more than upon the slowly varying drive speed V_d. It is therefore practical to measure belt velocity and obtain dynamic acceleration $2u^2/2t^2$ since the measurement is more sensitive than the slowly varying $2V_d/2t$.

5. Calculation of Belt Transient Tension from Belt Velocity Measurement

5.1 Experimental setup

The velocity of the conveyor belt during the starting and stopping period is measured using a low-cost miniature d.c. electric motor operating as a linear generator, converting belt velocity to voltage. The motor is connected by a 10.8:1 gearbox to a 7.5 cm diameter wheel contacting the belt edge. The voltage generated by the sensor when the belt moves is applied to an fm tape recorder and a chart recorder.

The acceleration of the belt with time is obtained by electronically differentiating the output of the velocity-speed S_1. Fig. 4 illustrates the system used to record belt velocity v(x,t) and belt acceleration a(x,t).

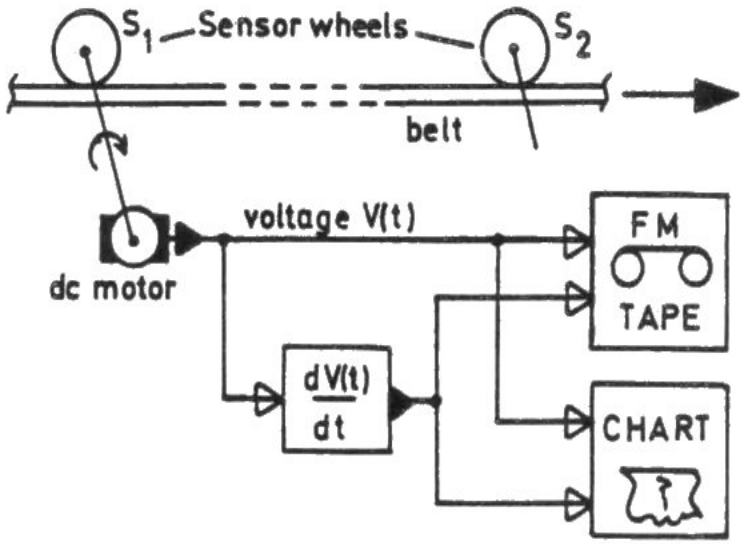

Fig. 4. Belt velocity transducers
with signal processing and recording
system shown for one transducer.

5.2 Transient tension calculation

The transient tension $T_d(x,t)$ in the belt is calculated using the experimentally derived value of in-plane belt acceleration a(x,t) and the relation

$$T_d(x,t) = m^* \cdot \frac{dv(x,t)}{dt} = m^*.a(x,t) \quad (9)$$

where m* is the effective mass opposing the motion of the travelling wave front, and is analogous to the electrical impedance of a transmission line. It was shown previously by calculating the kinetic energy of the elastic wave that the effective mass over 1 cycle of the fundamental velocity mode is m* = m/4 (3). The transient stress in the conveyor belt at a given location x at a time t is derived by dividing the value of T_d (x,t) by the total cross-sectional area of steel-cords. it is more convenient to calculate T_d values since these relate to f.o.s. requirements in belt system design.

6. Application

Fig. 5 illustrates one example of a belt conveyor system showing starting and stopping transients of belt velocity and calculated tension. These transients are directly attributed to travelling elastic

waves in the belt and the mass-spring effect provides only a small contribution to the acceleration and tension values. In this example, the belt length is l= 5.1 km, the belt weights 40 kg/m, the takeup mass M is 20000 kg, the belt stiffness is 10400 N/m and m is 398100 kg unloaded belt and 800000 kg loaded belt.

Fig. 5(a) shows the measured belt velocity during the starting and stopping period with a sensor S_1 placed on the return belt. Fig. 5(b) is the derived belt acceleration.

Fig. 5(c) shows the decaying elastic waves in the belt with a measured period t_1 = 7s, giving an elastic wave velocity of 1450 m/s. This compares favourably with the theoretical value of V_o = 1464 m/s calculated from equation (2) for the belt where ρ_S is 9 kg/m ρ_b is 40 kg/m and $\rho_i + \rho_m$ is 39 kg/m. The value of V_o was further confirmed by measuring the time delay between two sensors S_1 and S_2 spaced apart on the belt (Fig. 4). Fig. 5(d) illustrates the oscillation period of the takeup mass and the spring effect of the belt. The measured period of oscillation is 25 s. The theoretical value using equation (7) is t = 24 s for the unloaded belt. In the loaded belt the material mass severely damps the mass-spring effect.

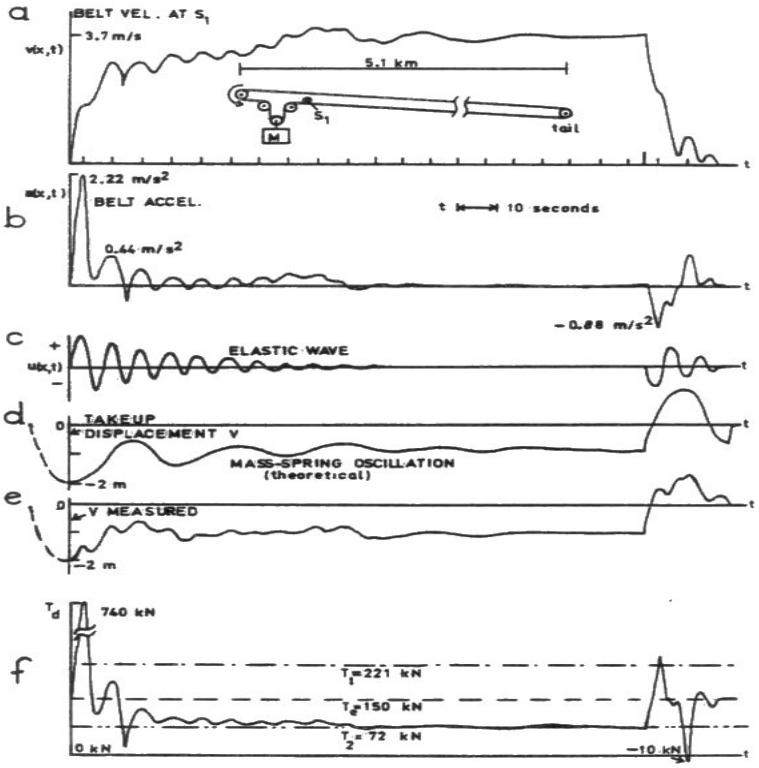

Fig. 5. Starting and stopping characteristics for a 5.1 km long conveyor belt.

1. Measured belt return-side velocity.
2. Derived in-plane belt acceleration.
3. Elastic wave compressions and rare-fractions causing perturbation to the belt speed at the drive drum. Measured wave period is 7 s.
4. Calculated mass-spring effect for the belt.
5. Mass-takeup motion showing the combined effects of the elastic travelling waves and the system's natural frequency due to the mass-spring effect.
6. Calculated transient tension superimposed on the normal running belt tension (belt loaded).

Fig. 5(e) illustrates the displacement of the mass takeup with time. It is obvious that the perturbation in belt velocity is synchronous with the motion of the mass, and this effect would be less pronounced if the takeup mass were at the tail end of the belt.
Fig. 5(f) illustrates the practical application of equation (9) in determining the transient tension in the belt return run. The peak calculated tension is 370 kN, which represents an instant f.o.s. of 6:1 for the unloaded belt and 3:1 for the loaded belt. A "soft" start with a peak belt acceleration of 0.5 m/s² would lead to a belt tension of 200 kN peak which happens to equal the running T1 tension. However for a belt f.o.s. of 6:1, it is only necessary to install a belt of strength ~SR1200, instead of the value used in this system of SR2250. The reduction in belt strength results in significant cost reduction. This can be achieved with the aid of controlled starting that reduce the shock(jerk) wave intensity. The same approach may be applied to braking a belt conveyor. Tail driven belts with full material loads can develop negative tension (compression) in the return span when rapid braking is applied to the belt. The belt sags at first, followed by severe whip caused by the tension wave in the carrying span arriving at the return span. This type of behaviour severely stresses the belt and can cause structure alignment problems and pulley bearing failure (4)

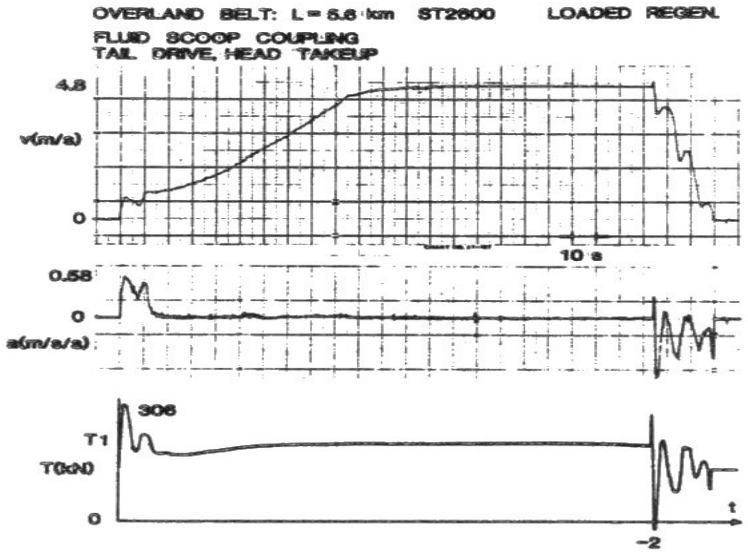

Fig. 6. illustrates the velocity characteristics for a fluid scoop coupled long overland conveyor belt. The origin of the elastic wave stems from the tail drive used. The elastic wave propagates along the return, encounters the loaded belt and slows down, causing a rapidly damped wave. Upon the application of the brakes, the belt sags on the return span due to compressive forces (negative tension), and reaches -2 kN.

7. Design Objectives

The previous example is similar in principle to many long conveyor belts in service. investigation of the transient behaviour at starting and stopping for many belt systems indicates that high stresses are generated in the belt. Multistep starting generates large tensions in the belt and fluid coupling drives stress the belt least. Braking conveyor belts normally generate the highest belt stresses. These large stresses stem from poorly designed starting and braking methods and result in the requirement of high f.o.s. in the belt. This is a costly and unnecessary practice.
In order to reduce belt f.o.s., and hence belt cost, the transient stress must be lowered. For existing systems such as in fig. 5 and 6, we can calculate the transient stress using equation (9). It is possible to modify start and stop durations, remeasure stress in the belt and when it is necessary to replace the belt, a lower f.o.s. can be used based on the peak stress measurements.
However, no design criteria exist in the literature for optimal starting and stopping of belts (5). The velocity, acceleration and jerk should be zero at time t = 0 and after the belt has reached full speed. The boundary conditions for the design are

Design Boundary Conditions:

vel	accel	jerk	
.		...	
$U=0$	$\ddot{U}=0$	$\dddot{U}=0$	$t=0$
.		...	
$U=V_b/2$	$\ddot{U}=a_{max}$	$\dddot{U}=0$	$t=T/2$
.		...	
$U=V_b$	$\ddot{U}=0$	$\dddot{U}=0$	$t \geq T$

(10)

and the starting or stopping characteristic which gives symmetric and least peak acceleration is

$$V(t) = V_b \cdot \frac{(1 - \cos \alpha t)}{2} \; ; \; 0 \leq t \leq T, \; \alpha = \frac{\pi}{T}$$
$$= V_b \qquad ; t \geq T \qquad (11)$$

The shape of the velocity-time characteristic of equation (11) is given in Fig. 7. The characteristic is known as a cycloidal-front, often used in engineering simulation (2). Using this function as a velocity-time drive curve, the peak acceleration at t = t/2 is, by differentiating equation (11),

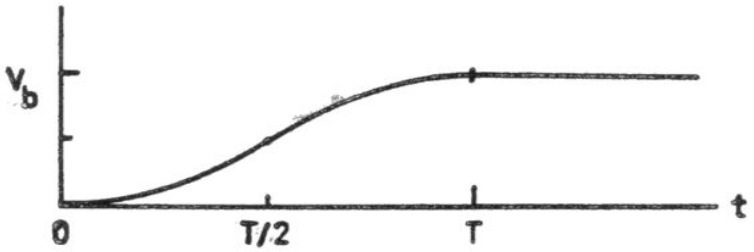

Fig. 7. Start or stop characteristic
to minimise stress in the belt, showing
belt velocity as a function of time.

$$a_{max} = \frac{V_b}{2} \cdot \frac{\pi}{T} \qquad (12)$$

where T is chosen to be the time to accelerate the belt to velocity Vb. The propagation of stress still applies here, and the peak transient non-oscillatory stress can be obtained by substituting equation (12) into equation (9), i.e. $T_d = m^* . a_{max}$.
Fig. 8 describes a speed controller to take advantage of the optimal speed curve using a programmable commercially available unit. The belt speed is sensed to ensure that drive overspeed does not occur.
From a belt point of view, the f.o.s. can be completely predetermined using this approach. Assuming that a steel-cord belt is designed to operate midway along its linear force-extension curve, then in terms of the breaking force B(kN), the operating load is 1/3. B.
Using the accepted f.o.s. definition in the introduction, the design f.o.s. to include dynamics should be calculated from

$$\text{f.o.s.} \geq 3\left(1 + \frac{m^* . \frac{Vb}{\pi}}{\sqrt{\frac{2T}{T_1}}}\right) \qquad (13)$$

where T_1 is the non-transient peak loaded tension in the belt. For example, if T_1 = 300 kN, m* = 200,000 kg, V_b = 6 m/s and we select a starting time of T = 55 sec, then f.o.s. $\geq$ 3.34:1. This means that an SR1000 steel-cord belt will operate successfully in this design, at less cost than a belt using classical f.o.s. values of 6.67:1 (SR2250) from the manufacturers handbooks.

BELT SPEED CONTROL

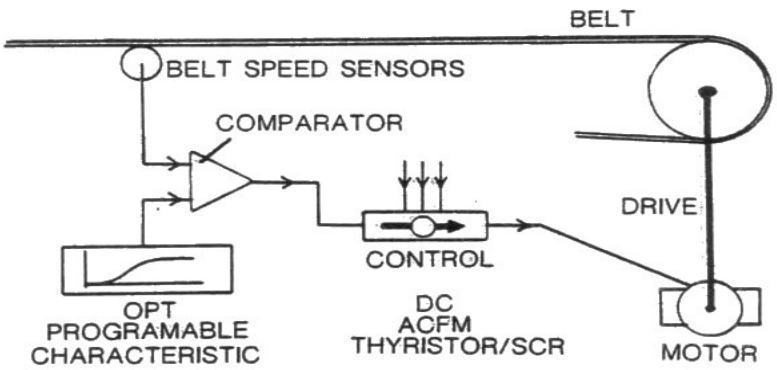

Fig. 8. Belt speed control to utilise programmable drive techniques.

8. Summary

Fig. 9. summarises a series of simulated starting characteristics for conveyor belts. The starting characteristic which provides the least jerk is given in fig. 9(f). This curve is continuous everywhere (no infinite jerk) and has zero acceleration at time t = 0 and after a selected period T. The acceleration curve is symmetrical, giving equally distributed positive and negative jerk of small amplitudes. A belt speed characteristic using the curve in fig. 9(f) at starting and stopping will stress the belt least by comparison to the alternative curves given in fig. 9. The curve is easily implemented with modern electronic controllers. The belt acceleration can be pre-selected and the peak tension pre-calculated. The effect of jerk on belt speed can be predicted, as in fig. 7.

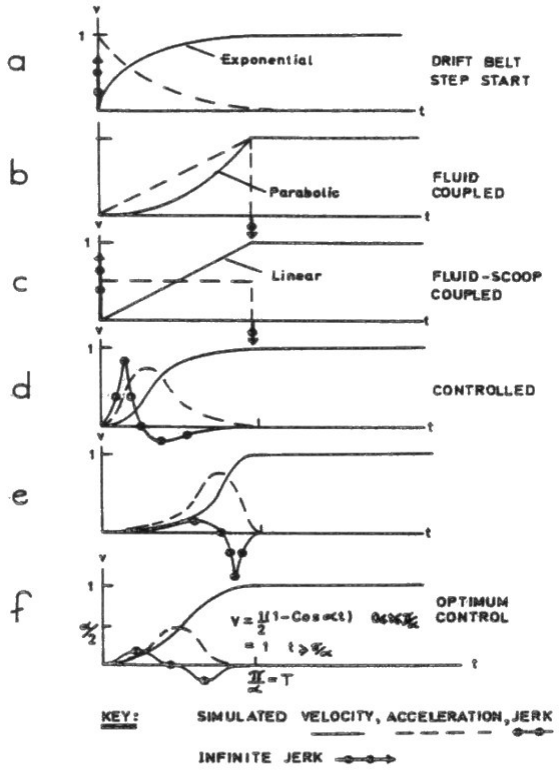

Fig. 9(a-e) Simulated speed curves for driving conveyor belts.

Fig. 9(f) An optimum curve for starting belt conveyors using part of a cosine curve. The acceleration amplitude in the belt is predictable at α/2 and this is governed by the required run-up or run-down time.

9. Conclusion

The design approach described provides an improved method for evaluating the f.o.s. for existing belt systems. Potentially over-stressed belts can be monitored and improved starting and stopping implemented. The belt f.o.s. for a new installation can be calculated in advance using the above methods. The application of correctly controlled starting and braking characteristics will considerably reduce the required f.o.s. for the belt and the system cost will be considerably reduced.

These methods may be further applied to the design of starting and stopping characteristics for fast belts (> 15 m/s), ensuring minimal transient stresses in the belt. Similarly, increasing the speed of existing belts may be achieved safely by correct belt speed control.

References

1. R.M. Davies: Stress waves in solids. Appl. Mech. Revs. Vol. 6 (1953) , 1-3.
2. S. Timoshenko, D.H. Young and W. Weaver.Vibration problems in Engineering, 4th Ed. John wiley 1974.
3. J.L. Goldberg, N.H. Clark and B.H. Meldrum: Application of tuned-mass dampers to the suppression of vibration. Shock and Vibration Bulletin No. 50, Part 4, p. 59. 1980.
4. A. Harrison: Dynamic behaviour of steel-cord conveyor belts. Colliery Guardian. Vol. 229 No. 9 (1981) page 459.
5. A. Harrison: Transient stresses in long conveyor belts. Proc. Belt conveying of Bulk Solids, Newcastle, Nov. 1982.